



# High-order accurate Lagrange-remap hydrodynamic schemes on staggered Cartesian grids

Gautier Dakin, Bruno Desprès, Stéphane Jaouen, Hervé Jourden

## ► To cite this version:

Gautier Dakin, Bruno Desprès, Stéphane Jaouen, Hervé Jourden. High-order accurate Lagrange-remap hydrodynamic schemes on staggered Cartesian grids. CEA GAMNI, Jan 2016, Paris, France. , 2016. hal-01280732

**HAL Id: hal-01280732**

**<https://hal.science/hal-01280732>**

Submitted on 2 Mar 2016

**HAL** is a multi-disciplinary open access archive for the deposit and dissemination of scientific research documents, whether they are published or not. The documents may come from teaching and research institutions in France or abroad, or from public or private research centers.

L'archive ouverte pluridisciplinaire **HAL**, est destinée au dépôt et à la diffusion de documents scientifiques de niveau recherche, publiés ou non, émanant des établissements d'enseignement et de recherche français ou étrangers, des laboratoires publics ou privés.





## High-order accurate Lagrange-remap hydrodynamic schemes on staggered Cartesian grids

Gautier Dakin<sup>††</sup>, Bruno Després<sup>†</sup>, Stéphane Jaouen<sup>‡</sup>, Hervé Jourden<sup>‡</sup>  
<sup>†</sup> Université Pierre et Marie Curie, LJLL, 4 pl Jussieu 75005 Paris, France  
<sup>‡</sup> CEA, DAM, DIF, F-91 297 Arpajon, France  
daking@ocre.cea.fr

CEA-GAMNI 2016



### Abstract

We consider a class of staggered grid schemes for solving the 1D Euler equations in internal energy formulation. The proposed schemes are applicable to arbitrary equations of state and high-order accurate in both space and time on smooth flows. Adding a discretization of the kinetic energy equation, a high-order kinetic energy synchronization procedure is introduced, preserving globally total energy and enabling proper shock capturing. Extension to 2D Cartesian grids is done via C-type staggering and high-order dimensional splitting. Numerical results are provided up to 8th order accuracy. Stability and reconstruction procedure for boundary conditions is then discussed.

### Introduction

In the late 1940s, the first shock capturing hydrodynamic scheme by von Neumann and Richtmyer [9] was a staggered 1D Lagrange *explicit* scheme, formulated in internal energy with artificial viscosity and *2nd order accuracy* in space and time on smooth flows. In 1961, a key contribution to 1D Lagrange schemes was provided by Trulio and Trigger [7] who identified the lack of conservation of total energy with the original scheme and proposed an *implicit* conservative version, retaining spatial staggering, without temporal staggering. In the early 1970s, pioneered by DeBar, several multifluid Eulerian hydrocodes with interface reconstruction on 2D Cartesian grids [2, 6] relied on the Trulio-Trigger *implicit* Lagrangian scheme, making use of a Lagrange-remap approach with dimensional splitting. Later, a strictly *explicit* conservative version of the Trulio-Trigger scheme was reported in [10] on 2D Cartesian grids, in a 1D Lagrange-remap setting with Strang dimensional splitting. Recent works on staggered schemes as in [4] proposed a way of controlling kinetic energy for accurate shock capturing. In [1], we proposed an extension path of such schemes to high-order accuracy with a finite volume approach, combining high-order Runge-Kutta time integration in the Lagrange phase, high-order 1D spatial reconstructions and remap. We give in the following the mainline of such a path, and propose a short sight of stability and reconstruction of boundary conditions.

### 1D staggered Lagrange-Remap scheme

First, let us consider the 1D hydrodynamics system (1) closed with an arbitrary EOS such that  $p = EOS(\tau, \epsilon)$  where  $p = 1/\tau$ ,  $u$ ,  $p$ ,  $e$ ,  $\epsilon$ ,  $e_{kin} = u^2/2$  denote respectively the mass density, the velocity, the pressure and the total, internal and kinetic energies. Let us denote  $\rho_0$  the initial mass density. Introducing the change of variable  $(x, t) \rightarrow (X, t)$  satisfying  $pdx = \rho_0 dX$  and using  $e = \epsilon + e_{kin}$ , (1) rewrites (2) in Lagrangian coordinates:

$$\begin{cases} \partial_t p + \partial_x(\rho u) = 0 \\ \partial_t(\rho u) + \partial_x(\rho u^2 + p) = 0 \\ \partial_t(\rho e) + \partial_x(\rho u e + \rho u) = 0 \end{cases}, \quad (1) \quad \begin{cases} \partial_t(\rho_0 \tau) - \partial_X u = 0 \\ \partial_t(\rho_0 u) + \partial_X p = 0 \\ \partial_t(\rho_0 \epsilon) + p \partial_X u = 0 \\ \partial_t(\rho_0 e_{kin}) + u \partial_X p = 0 \end{cases}. \quad (2)$$

The principle of the Lagrange-remap approach selected here is to integrate in time the Lagrangian system (2) followed by a conservative remap of the variables on the initial grid. We consider a *primal* uniform Cartesian grid  $\{x_{i+\frac{1}{2}}\}$  with  $\Delta X = x_{i+\frac{1}{2}} - x_{i-\frac{1}{2}}$  and a *dual* grid  $\{x_i\}$  with  $x_i = \frac{1}{2}(x_{i+\frac{1}{2}} + x_{i-\frac{1}{2}})$ . In the following,  $\bar{\phi}$  and  $\phi$  will respectively denote the space averaged value of  $\phi$  and its point-wise value.

#### Lagrange step

We consider  $N$ th order *explicit* schemes with the following notations for Runge-Kutta sequences:  $\alpha_m$  is the time step for the  $m$ th sub-cycle,  $a_{m,l}$  the  $m, l$  term of the Butcher table and  $\theta_l$  the  $l$ th reconstruction coefficient for the last step. The artificial viscosity possibly applied for strong shocks is denoted  $q$  with  $\Pi = p + q$ .

$$\begin{cases} \overline{\rho_0 \tau_i^{n+\alpha_m}} = \overline{\rho_0 \tau_i^n} + \frac{\Delta t}{\Delta X} \sum_{l=0}^{m-1} a_{m,l} d u_i^{n+\alpha_l} \\ \overline{\rho_0 u_{i+\frac{1}{2}}^{n+\alpha_m}} = \overline{\rho_0 u_{i+\frac{1}{2}}^n} - \frac{\Delta t}{\Delta X} \sum_{l=0}^{m-1} a_{m,l} d \Pi_{i+\frac{1}{2}}^{n+\alpha_l} \\ \overline{\rho_0 \epsilon_i^{n+\alpha_m}} = \overline{\rho_0 \epsilon_i^n} - \frac{\Delta t}{\Delta X} \sum_{l=0}^{m-1} a_{m,l} \overline{\Pi \delta u_i^{n+\alpha_l}} \\ x_{i+\frac{1}{2}}^{n+\alpha_m} = x_{i+\frac{1}{2}}^n + \Delta t \sum_{l=0}^{m-1} a_{m,l} u_{i+\frac{1}{2}}^{n+\alpha_l} \\ p_i^{n+\alpha_m} = EOS(\tau_i^{n+\alpha_m}, \epsilon_i^{n+\alpha_m}) \end{cases}, \quad (3) \quad \begin{cases} \overline{\rho_0 \tau_i^{n+1}} = \overline{\rho_0 \tau_i^n} + \frac{\Delta t}{\Delta X} \sum_{l=0}^{s-1} \theta_l d u_i^{n+\alpha_l} \\ \overline{\rho_0 u_{i+\frac{1}{2}}^{n+1}} = \overline{\rho_0 u_{i+\frac{1}{2}}^n} - \frac{\Delta t}{\Delta X} \sum_{l=0}^{s-1} \theta_l d \Pi_{i+\frac{1}{2}}^{n+\alpha_l} \\ \overline{\rho_0 \epsilon_i^{n+1}} = \overline{\rho_0 \epsilon_i^n} - \frac{\Delta t}{\Delta X} \sum_{l=0}^{s-1} \theta_l \overline{\Pi \delta u_i^{n+\alpha_l}} \\ \overline{\rho_0 e_{kin,i+\frac{1}{2}}^{n+1}} = \overline{\rho_0 e_{kin,i+\frac{1}{2}}^n} - \frac{\Delta t}{\Delta X} \sum_{l=0}^{s-1} \theta_l u \delta \Pi_{i+\frac{1}{2}}^{n+\alpha_l} \\ x_{i+\frac{1}{2}}^{n+1} = x_{i+\frac{1}{2}}^n + \Delta t \sum_{l=0}^{s-1} \theta_l u_{i+\frac{1}{2}}^{n+\alpha_l} \\ p_i^{n+1} = EOS(\tau_i^{n+1}, \epsilon_i^{n+1}) \end{cases}, \quad (4)$$

where  $d\phi$  is the difference between consecutive *point-wise* values:  $d\phi_i = \phi_{i+\frac{1}{2}} - \phi_{i-\frac{1}{2}}$  and  $d\phi_{i+\frac{1}{2}} = \phi_{i+1} - \phi_i$ .

To achieve high-order resolution, it is mandatory to compute the point-wise (resp. average) values from the average (resp. point-wise) ones with high-order accuracy. Although other reconstructions may be used, centered and symmetric ones are sufficient for *uniform* Cartesian grids.

$$\begin{cases} \phi_{\xi(i)} = \sum_k C_k \bar{\phi}_{\xi(i)+k} \\ \bar{\phi}_{\xi(i)} = \sum_k \hat{C}_k \phi_{\xi(i)+k} \\ \delta \phi_{\xi(i)} = \sum_{k \geq 0} d_k \left( \phi_{\xi(i)+k+\frac{1}{2}} - \phi_{\xi(i)-k-\frac{1}{2}} \right) \end{cases}, \quad \begin{cases} \phi_{\xi(i)} = \sum_k Q_{k+\frac{1}{2}} \bar{\phi}_{\xi(i)+k+\frac{1}{2}} \\ \bar{\phi}_{\xi(i)} = \sum_k \hat{Q}_{k+\frac{1}{2}} \phi_{\xi(i)+k+\frac{1}{2}} \end{cases}, \quad \text{with } \xi(i) = \begin{cases} i & \text{on primal grid} \\ i + \frac{1}{2} & \text{on dual grid} \end{cases}. \quad (5)$$

### Lemma

For all Runge-Kutta sequences, all artificial viscosities, all spatial reconstructions, the schemes (3-5) formulated in internal energy are conservative in mass, momentum and total energy.

### Proof.

Conservation of mass and momentum is immediate, we only prove the conservation of total energy.

$$\begin{aligned} \Delta E &= \sum_i \left( \overline{\rho_0 e_{tot,i}^{n+1}} - \overline{\rho_0 e_{tot,i}^n} \right) = \sum_i \left( \overline{\rho_0 \epsilon_i^{n+1}} - \overline{\rho_0 \epsilon_i^n} \right) + \sum_i \left( \overline{\rho_0 e_{kin,i+\frac{1}{2}}^{n+1}} - \overline{\rho_0 e_{kin,i+\frac{1}{2}}^n} \right) = -\frac{\Delta t}{\Delta X} \sum_i \sum_{l=1}^s \theta_l \left( \overline{\Pi \delta u_i^{n+\alpha_l}} + \overline{u \delta \Pi_{i+\frac{1}{2}}^{n+\alpha_l}} \right) \\ &= -\frac{\Delta t}{\Delta X} \sum_i \sum_{l=1}^s \sum_k \sum_{k'} \theta_l \hat{C}_k d_k \left( \Pi_{i+k}^{n+\alpha_l} u_{i+k+k'+\frac{1}{2}}^{n+\alpha_l} + u_{i+k+\frac{1}{2}}^{n+\alpha_l} \Pi_{i+k+k'+1}^{n+\alpha_l} - \Pi_{i+k}^{n+\alpha_l} u_{i+k-k'-\frac{1}{2}}^{n+\alpha_l} - u_{i+k+\frac{1}{2}}^{n+\alpha_l} \Pi_{i+k-k'}^{n+\alpha_l} \right). \end{aligned}$$

Making the change of index  $i \leftarrow i + k'$  in the first term and  $i \leftarrow i + k' + 1$  in the second term of the RHS we get the result for wall (with non-trivial definitions of ghost-cell values) or periodic boundary conditions.

$$\Delta E = -\frac{\Delta t}{\Delta X} \sum_i \sum_{l=1}^s \sum_{k,k'} \theta_l \hat{C}_k d_k \left( \Pi_{i+k-k'}^{n+\alpha_l} u_{i+k+\frac{1}{2}}^{n+\alpha_l} + u_{i+k-k-\frac{1}{2}}^{n+\alpha_l} \Pi_{i+k}^{n+\alpha_l} - \Pi_{i+k}^{n+\alpha_l} u_{i+k-k'-\frac{1}{2}}^{n+\alpha_l} - u_{i+k+\frac{1}{2}}^{n+\alpha_l} \Pi_{i+k-k'}^{n+\alpha_l} \right) = 0.$$

### Remap step

After the Lagrange step, the dual deformed grid  $\{x_i^{n+1}\}$  is computed by high-order interpolation of the primal deformed grid  $\{x_{i+\frac{1}{2}}^{n+1}\}$  as  $x_i = \sum_{k \geq 0} r_k \left( x_{i+k+\frac{1}{2}} + x_{i-k-\frac{1}{2}} \right)$ . All variables  $(\rho\phi)$  for  $\phi \in \{1, \epsilon\}$  are remapped on the primal grid  $\{x_{i+\frac{1}{2}}\}$  and for  $\phi \in \{1, u, e_{kin}\}$  on the dual grid  $\{x_i\}$  according to :

$$\overline{\rho\phi_i^{n+1}} = \frac{1}{\Delta X} \int_{x_{i-\frac{1}{2}}}^{x_{i+\frac{1}{2}}} \rho\phi(x, t^{n+1}) dx = \frac{1}{\Delta X} \left[ \int_{x_{i-\frac{1}{2}}}^{x_{i+\frac{1}{2}}} \rho\phi dx + \int_{x_{i+\frac{1}{2}}^{n+1}}^{x_{i+\frac{1}{2}}} \rho\phi dx + \int_{x_{i+\frac{1}{2}}^{n+1}}^{x_{i+\frac{1}{2}}} \rho\phi dx \right],$$

written in *conservative* flux-form:

$$\overline{\rho\phi_i^{n+1}} = \overline{\rho\phi_i^{n+1}} - \left[ \frac{x_{i+\frac{1}{2}}^{n+1} - x_{i+\frac{1}{2}}}{\Delta X} (\rho\phi)_{i+\frac{1}{2}}^* - \frac{x_{i-\frac{1}{2}}^{n+1} - x_{i-\frac{1}{2}}}{\Delta X} (\rho\phi)_{i-\frac{1}{2}}^* \right]. \quad (6)$$

To compute  $(\rho\phi)_{i+\frac{1}{2}}^*$ , we use the high-order Lagrange polynomial  $P_{up}^\phi$  interpolating point-wise values of  $H_{up}^\phi(X) = \int_{-x_{up-\frac{N}{2}+\frac{1}{2}}}^X (\rho\phi)(y) dy$  on the deformed grid, with a stencil of length  $(N+1)$  leading to:

$$(\rho\phi)_{i+\frac{1}{2}}^* = \frac{1}{x_{i+\frac{1}{2}}^{n+1} - x_{i-\frac{1}{2}}^{n+1}} (P_{up}^\phi(x_{i+\frac{1}{2}}^{n+1}) - P_{up}^\phi(x_{i-\frac{1}{2}}^{n+1})), \text{ where } up = \begin{cases} i & \text{if } x_{i+\frac{1}{2}}^{n+1} > x_{i+\frac{1}{2}} \\ i+1 & \text{otherwise} \end{cases}. \quad (7)$$

### Point-wise kinetic energy synchronization step

A high-order accurate synchronization is introduced on point-wise kinetic energies according to (8).

- Compute the difference  $\Delta K$  between point-wise *remapped* kinetic energy and point-wise *reconstructed* kinetic energy.
  - Distribute  $\Delta K$  on the average values of kinetic energy and internal energy on the stencil.
- $$\begin{cases} \Delta K_{i+\frac{1}{2}} = \rho e_{kin,i+\frac{1}{2}}^{n+1} - \frac{1}{2} \frac{(\rho u)_{i+\frac{1}{2}}^{n+1}}{\rho_{i+\frac{1}{2}}^{n+1}} \\ \overline{\rho e_{kin,i+\frac{1}{2}}^{n+1}} \leftarrow \overline{\rho e_{kin,i+\frac{1}{2}}^{n+1}} - \sum_k \hat{C}_k \Delta K_{i+k+\frac{1}{2}} \\ \overline{\rho \epsilon_i^{n+1}} \leftarrow \overline{\rho \epsilon_i^{n+1}} + \sum_k \hat{Q}_{k+\frac{1}{2}} \Delta K_{i+k+\frac{1}{2}}. \end{cases} \quad (8)$$

### Lemma

The kinetic energy synchronization procedure is conservative in total energy.

### Proof.

For wall (still with non trivial definitions of ghost-cell values) or periodic boundary conditions, we have:

$$\Delta E = \sum_i \left( \sum_{k'} \hat{Q}_{k'+\frac{1}{2}} \Delta K_{i+k'+\frac{1}{2}} - \sum_k \hat{C}_k \Delta K_{i+k+\frac{1}{2}} \right) = 0.$$

### 2D Extension

The 1D schemes (3-8) are now to be used with a dimensional splitting method (DSM) on the 2D system

$$\begin{cases} \partial_t \rho + \nabla \cdot (\rho \vec{u}) = 0, \\ \partial_t(\rho \vec{\Phi}) + \nabla \cdot (\rho \vec{\Phi} \otimes \vec{u} + \vec{f}) = 0, \end{cases} \quad \text{with } \vec{\Phi} = \begin{pmatrix} \vec{u} \\ e \end{pmatrix} \text{ and } \vec{f} = \begin{pmatrix} p_n \\ \rho \vec{u}^t \end{pmatrix}. \quad (9)$$

A C-type staggering is retained: variables are indexed  $\phi_{i,j}$  for  $\phi \in \{\rho_0, \rho_0 \tau, \rho_0 \epsilon\}$ ,  $\phi_{i+\frac{1}{2},j}$  for  $\phi \in \{\rho_0, \rho_0 u, \rho_0 e_{kin,u}\}$  and  $\phi_{i,j+\frac{1}{2}}$  for  $\phi \in \{\rho_0, \rho_0 v, \rho_0 e_{kin,v}\}$ . As previous 1D schemes are based on a 1D finite volume formulation, it is mandatory to add a transverse interpolation to deduce 1D-cell-average values from 2D-cell-average ones. The procedure originates from [3] extended here to staggered grids. A sweep along the x-direction proceeds as follows:

- Interpolate along the y-direction to get 1D-cell-average values of the conservative variables according to (5). This way, we only get 1D-cell-average values along the x-direction.
- Apply the 1D Lagrange scheme with extra equations for  $v$  contributions to momentum and kinetic energy ( $\partial_t \rho_0 v = \partial_t \rho_0 e_{kin,v} = 0$ ). Remap must be performed on three different grids.
- Reconstruct the 2D fluxes from the 1D Lagrange and remap fluxes according to (5).
- Apply the reconstructed 2D fluxes on 2D-cell-average values.

### Lemma

The resulting 2D Cartesian grid schemes are conservative in mass, momentum and total energy.

### Proof.

With the C-type staggering of variables, the 2D schemes verify Lemmas 1 and 2 direction by direction and so are globally conservative in mass, momentum and total energy for all dimensional splitting.  $\square$

### Numerical Results

No artificial viscosities/hyperviscosities nor limiters are used in the Lagrange and remap steps. The point-wise kinetic energy synchronization procedure is applied on all cases.

The Shu-Osher test case [5] is initialized as (10) on a  $[-5 : 5]$  domain with a Mach 3 shock wave interacting with a sinusoidal density field. Computations till  $t=1.8$  with  $CFL = 0.2$  are reported in Figure 1(a) and highlight the robustness and high resolution of the 6th and 9th order schemes with only 200 cells.

The 2D vortex advection test case is used to assess the accuracy of the schemes under IEEE-754 norm for double precision. The initial condition is given by (11). Computations are performed on a  $[-10 : 10]^2$  domain till  $t=1$  with  $CFL = 0.9$ ,  $\gamma = 1.4$  and  $\beta = 5$ . The  $L^1$ -errors in both space and time are computed as  $err_{L^1} = \sum_n \Delta t^n \cdot \Delta x \cdot \Delta y \sum_{i,j} \|\rho \Phi_{i,j}^{(n)} - \rho \Phi_{i,j}^{(n)}(t^n)\|_{L^1}$  with  $\Phi = (1, \vec{u}, e)^t$  and reported on Figure 1(b) with excellent agreement to expected orders.

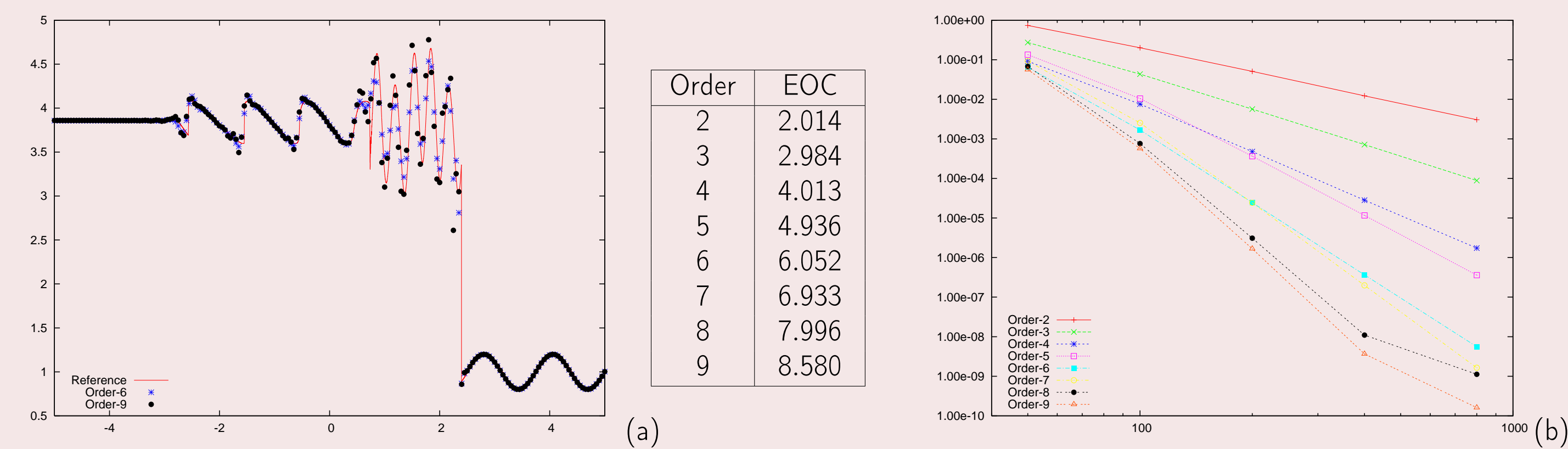


Figure : (a) Shu-Osher test case on 200 cells for the 6th and 9th order schemes. (b) Experimental order of convergence (EOC) on the 2D advected vortex test case from 2nd to 9th-order and  $L^1$ -error in both space and time with respect to the number of cells per direction.

$$(\rho_0, u_0, p_0) = \begin{cases} \left( \frac{27}{7}, \frac{4\sqrt{35}}{7}, \frac{31}{7} \right) & \text{if } x \in [-5 : -4[ \\ \left( 1 + \frac{\sin(\frac{5x}{2})}{5}, 0, 1 \right) & \text{if } x \in [-4 : 5] \end{cases} \quad (10) \quad \begin{cases} \rho_0 = \left( 1 - \frac{(\gamma-1)\beta^2}{8\gamma\pi^2} e^{1-r^2} \right)^{\frac{1}{\gamma-1}} \\ \vec{u}_0 = \vec{1} + \frac{\beta}{2\pi} e^{\frac{1-r^2}{2}} \cdot (-y, x)^t \\ p_0 = \rho_0^{\frac{2}{\gamma}} \end{cases} \quad (11)$$

### Local stability of boundary conditions

In this part, we attempt to determine a form of local stability criterion for problem with non-periodic boundary conditions.

Let  $\mathcal{U} = (u_j)_{j \in \mathbb{Z}}$ ,  $\mathcal{U}^+ = (u_j)_{j \geq 1}$ ,  $\mathcal{U}^- = (u_j)_{j \leq 0}$ .

- Let  $\mathcal{M} : \mathbb{R}^{\mathbb{Z}} \rightarrow \mathbb{R}^{\mathbb{Z}}$  be the band-matrix of the interior scheme such that  $\overline{\mathcal{U}} = \mathcal{M}\mathcal{U}$  and suppose  $M$  to be unitary stable:

$$\|\mathcal{M}\mathcal{U}\|_l \leq \|\mathcal{U}\|_p \quad (12)$$

- Let  $\mathcal{R} : \mathbb{R}^{\mathbb{N}} \rightarrow \mathbb{R}^{\mathbb{N}}$  define a reconstruction procedure such that :

$$\mathcal{U}^- = \mathcal{R}\mathcal{U}^+, \mathcal{R} = \begin{pmatrix} R & 0 \\ 0 & 0 \end{pmatrix} \quad (13)$$

Given  $\mathcal{M}$ , we forge  $\mathcal{R}$ , in a similar fashion as in [8] using Inverse-Law Wendroff boundary treatment, such that the order of convergence nor the stability will be altered by the boundary conditions and the reconstruction procedure. We consider the following equation to be solved

$$\partial_t \rho + \partial_x \rho = 0 \quad (14)$$

We consider a  $C^\infty$  test-case with entering mass boundary condition at the point  $x_s$  which is not mandatorily a point of the mesh. The initial data is set to zero and the boundary condition is set as described in (15)

$$\rho(x_s, t) = -e^{\frac{0.1}{t}} \sin(4\pi t) \quad (15)$$

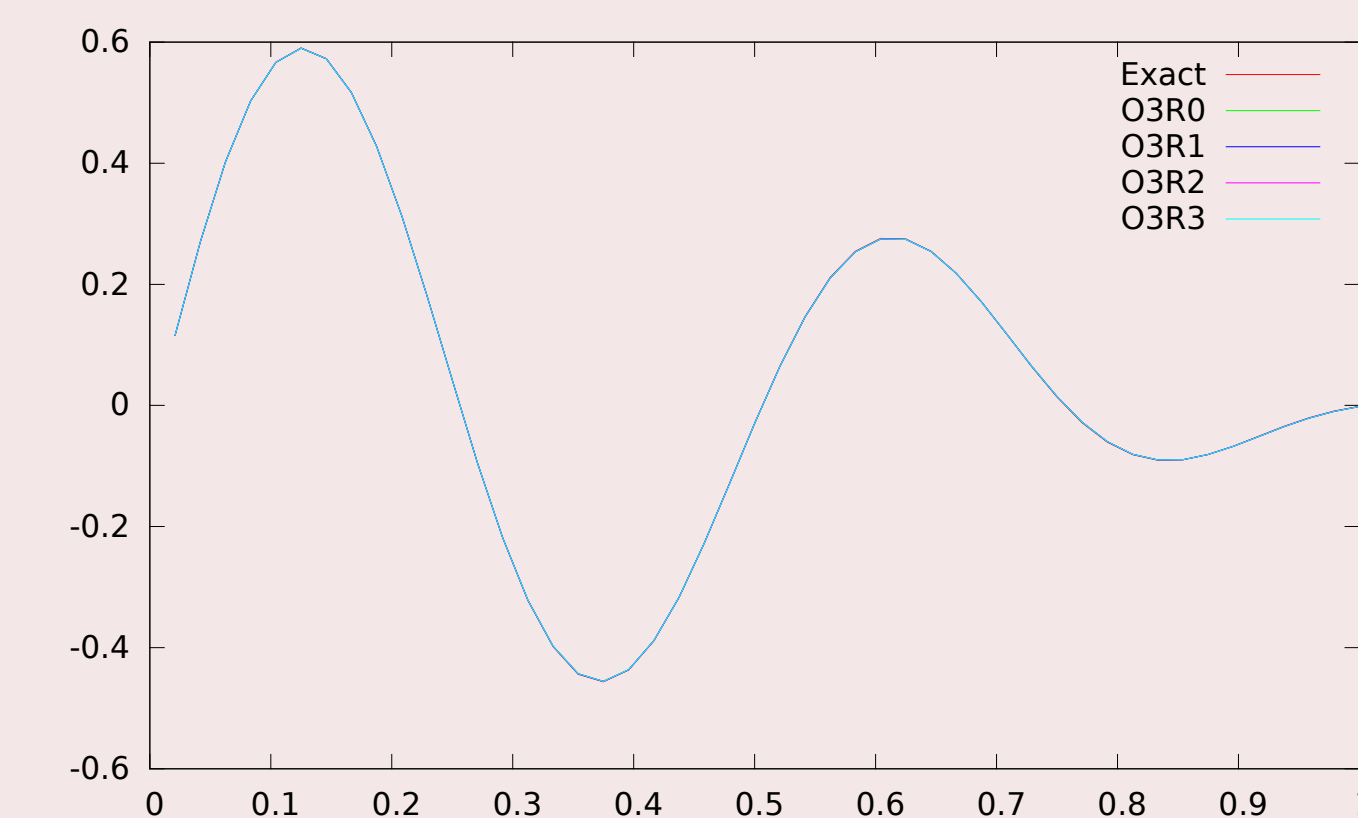


Figure : Computation performed until  $T = 1.5$  and  $L^1$ -error/EOC function of the number of cells for some reconstructions  $\mathcal{R}$  with non trivial boundary conditions with a third-order projection scheme

A standard procedure is developed which is stable without any CFL restriction, consistent to the desired order for all boundary conditions and for all point  $x_s$ .

### References

- [1] Dakin, G. and Jourden, H. (2016). High order conservative Lagrange-remap schemes on staggered Cartesian grids for compressible hydrodynamics. *C. R. Acad. Sci. Paris, Ser. I*, ??:??
- [2] DeBar, R. B. (1974). Fundamentals of the KRAKEN code. *Lawrence Livermore Laboratory Report*, Technical Report UCIR-760.
- [3] Duboc, F., Enaux, C., Jaouen, S., Jourden, H., and Wolff, M. (2010). High-order dimensionally split Lagrange-remap schemes for compressible hydrodynamics. *C. R. Acad. Sci. Paris, Ser. I*, 348:105–110.
- [4] Herbin, R. and Latché, J.-C. (2010). Kinetic energy control in the MAC discretization of compressible Navier-Stokes equations. *International Journal of Finite Volume*, 7(2):electronic.
- [5] Shu, C.-W. and Osher, S. (1989). Efficient Implementation of Essentially Non-oscillatory Shock-capturing Schemes, II. *J. Comput. Phys.*, 83:32–78.
- [6] Sutcliffe, W. G. (1974). BBC hydrodynamics. *Lawrence Livermore Laboratory Report*, Technical Report UCID-17013.
- [7] Trulio, J. G. and Trigger, K. R. (1961). Numerical solution of the one dimensional Lagrangian hydrodynamics equations. *Lawrence Radiation Laboratory Report*, Technical Report UCRL-6267.
- [8] Vilar, F. and Shu, C.-W. (2014). Development and stability analysis of the inverse Lax-Wendroff boundary treatment for central compact schemes. *ESAIM: Mathematical Modelling and Numerical Analysis*, page Published online.
- [9] von Neumann, J. and Richtmyer, R. D. (1950). A method for numerical calculation of hydrodynamic shocks. *J. Appl. Phys.*, 21:232–237.
- [10] Woodward, P. and Colella, P. (1984). The numerical simulation of two-dimensional fluid flow with strong shocks. *J. Comput. Physics*, 54:115–173.